THE ASTROPHYSICAL JOURNAL, 243:700–709, 1981 February 1

RELATIVISTIC JETS AS X-RAY AND GAMMA-RAY SOURCES[1]

ARIEH KÖNIGL
W. K. Kellogg Radiation Laboratory, California Institute of Technology
Received 1980 June 4; accepted 1980 August 13

ABSTRACT

The radio-through-γ-ray emission from beamed relativistic jets associated with bright, compact radio sources is considered and applied to the interpretation of extragalactic X-ray and γ-ray sources. It is argued that in sources which are viewed at small angles to their jet axes, the beamed emission component also contributes significantly to the observed X-ray and γ-ray radiation. Model synchrotron and inverse-Compton spectra for a resolved jet and for an unresolved inhomogeneous jet are calculated, taking into account the effect of synchrotron radiation losses. It is shown how the source nonuniformity in an unresolved jet gives rise to a spectrum which may be quite different from the local emission spectrum in both the optically thick and the optically thin regimes. On the basis of this model, it is pointed out that various observed features in the spectra of BL Lac objects could be attributed to emission from unresolved relativistic jets. The spectrum of 3C 273 is discussed, and it is concluded that the infrared-through-X-ray flux is probably unbeamed, but that the radio emission and perhaps also the high-energy γ-rays are beamed from the relativistic radio jet associated with this source. It is argued that if 3C 273 is a typical quasar, then a large fraction of the diffuse high-energy γ-ray background could be contributed by beamed sources. In addition, a synchrotron-radiation model is proposed for the resolved X-ray jet in Cen A.

Subject headings: BL Lacertae objects — gamma rays: general — quasars — radio sources: general — synchrotron radiation — X-rays: sources

I. INTRODUCTION

A growing number of extragalactic radio sources are being found to possess narrow, elongated features (jets) which connect the extended radio components with a central compact core. It is currently believed that these jets supply the extended components with matter and energy from a central "powerhouse," which is usually identified with a quasar or an active galactic nucleus (e.g., Blandford and Rees 1978*a*). The radio emission is generally interpreted as incoherent synchrotron radiation from a nonthermal distribution of relativistic electrons. Many strong compact sources also show evidence for relativistic bulk motion, most notably in apparent superluminal separation velocities of individual components (e.g., Cohen *et al.* 1979). In fact, it has been argued (Scheuer and Readhead 1979; Blandford and Königl 1979*b*, hereafter Paper I) that the majority of bright, compact radio sources could be identified with relativistic supersonic jets which are observed at small angles to their axes. In this picture, the sequence—radio-quiet quasars, radio-loud quasars, and "blazars" (i.e., optically violently variable quasars and BL Lac objects)—corresponds to similar strong sources, associated with relativistic jets, which are viewed at progressively smaller angles to their axes. As the angle of observation decreases, the contribution of the highly variable and strongly polarized beamed emission component increases relative to the steady and unpolarized isotropic component which is responsible for photoionizing the emission-line gas near the nucleus. Blazars are interpreted as sources in which the beamed component dominates the observed emission (cf. Angel and Stockman 1980).

Relativistic jets associated with compact radio sources are also expected to be X-ray and γ-ray sources, with synchrotron and inverse-Compton being the most likely emission mechanisms. Recent X-ray observations (e.g., Tananbaum *et al.* 1979; Ku 1980) have indicated that a substantial fraction of radio-selected quasars, and most blazars, are indeed X-ray sources, and that blazars can be highly variable also in the X-ray regime (e.g., Ricketts, Cooke, and Pounds 1976; Mushotzky *et al.* 1979). Furthermore, the only quasar identified so far as a high-energy ($\gtrsim 100$ MeV) γ-ray source is 3C 273 (Swanenburg *et al.* 1978), which is also a bright, compact radio source that displays apparent superluminal velocities (e.g., Cohen *et al.* 1979). When interpreted in the context of the relativistic-jet model, these observations appear to suggest that the beamed component also contributes significantly to the observed X-ray and γ-ray radiation in sources which are viewed at small angles to their jet axes. In this paper, the relativistic-jet model for compact radio sources is extended and applied to the interpretation of extragalactic X-ray and γ-ray sources. The synchrotron and inverse-Compton spectra of an inhomogeneous relativistic jet are calculated in § II on the basis of a simple emission model. This calculation generalizes the results of Paper I for the steady emission component in the jet. The model is then

[1] Supported in part by the National Science Foundation (AST78-05484).

applied in § III to the interpretation of the spectra of BL Lac objects and of 3C 273. In addition, the postulated local synchrotron spectrum is applied to the resolved X-ray jet in Cen A. Some general properties of extragalactic X-ray sources and the contribution of relativistic jets to the diffuse X-ray and γ-ray background are discussed in § IV. A summary of the results is given in § V.

II. SYNCHROTRON AND INVERSE-COMPTON EMISSION FROM A RELATIVISTIC JET

In this section, the synchrotron and inverse-Compton spectra are calculated for a resolved jet and for an unresolved inhomogeneous jet. The local synchrotron spectrum is described in § II*a*. It is assumed to be produced by a power-law distribution of continuously reaccelerated relativistic electrons and to break as a result of synchrotron radiation losses. The local synchrotron self-Compton spectrum is then calculated in the δ-function approximation. The corresponding spectra for an unresolved jet are obtained in § II*b* by adding up the contributions of the local emission spectra from the entire jet. In this calculation it is assumed that the relativistic-electron distribution has the same power-law throughout the source, but the coefficient of the distribution and the magnitude of the magnetic field in which the electrons radiate are allowed to vary along the jet.

a) Local Emission Spectrum

Consider a narrow conical jet of semiangle φ which has a constant velocity β_j (in units of the speed of light c) and which is seen at an angle θ ($\theta > \varphi$) to the axis. Assume that a portion of the jet at a distance r from the apex, subtending a solid angle $\Delta\Omega_{ob}$ at the observer, emits optically thin radiation at frequency ν' with spectral emissivity $\epsilon(\nu')$, as measured in the rest frame of the jet. The observed frequency is $\nu = \mathscr{D}_j \nu'/(1+z)$, where z is the redshift of the source and $\mathscr{D}_j = \gamma_j^{-1}(1 - \beta_j \cos\theta)^{-1}$, with $\gamma_j = (1-\beta_j^2)^{-1/2}$, is the relativistic Doppler factor. The observed flux density is then

$$S_{ob}(\nu) \approx (1+z)^{-3}\mathscr{D}_j^2(2r\varphi \csc\theta)(\Delta\Omega_{ob}/4\pi)\epsilon[(1+z)\nu/\mathscr{D}_j] . \quad (1)$$

(Note that the observed radius and cone angle are given by $r_{ob} = r \sin\theta$ and $\varphi_{ob} = \varphi \csc\theta$, respectively.)

The synchrotron emissivity ϵ_s due to relativistic electrons with a power-law distribution $n_e(\gamma_e) = K_e \gamma_e^{-(2\alpha_e+1)}$, $\gamma_{e\,min} \le \gamma_e \le \gamma_{e\,max}$, radiating isotropically in a magnetic field B, is given by

$$\epsilon_s[(1+z)\nu_s/\mathscr{D}_j] = (1+z)^{-\alpha_e}\mathscr{D}_j^{\alpha_e}\nu_s^{-\alpha_e}C_1(\alpha_e)K_e B^{1+\alpha_e} , \quad \nu_{s\,min} \le \nu_s \le \nu_{s\,max} , \quad (2)$$

where $[(1+z)\nu_s/\mathscr{D}_j]$ is the argument of ϵ_s, and where $C_1(\alpha_e)$ is a constant [e.g., Blumenthal and Gould 1970; $C_1(0.5) = 3.6 \times 10^{-19}$ cgs]. The spectral energy density of the optically thin radiation can be approximated by $[\epsilon_s(\nu_s')t_{es}']$, where $t_{es}' \approx r\varphi/c$ is the mean photon lifetime before escape. In what follows, it will be assumed that the relativistic electrons are injected continuously with $K_e = K$, $\alpha_e = \alpha_0$, and with Lorentz factors in the range $\gamma_{el} \le \gamma_e \le \gamma_{eu}$, but that α_e increases to $(\alpha_0 + 0.5)$ for $\gamma_e > \gamma_{eb}$ ($\gamma_{el} \ll \gamma_{eb} \ll \gamma_{eu}$) owing to synchrotron-radiation losses (see Kellermann 1966). The model synchrotron spectrum is illustrated in Figure 1. Below the frequency ν_{sm} the source is optically thick to synchrotron

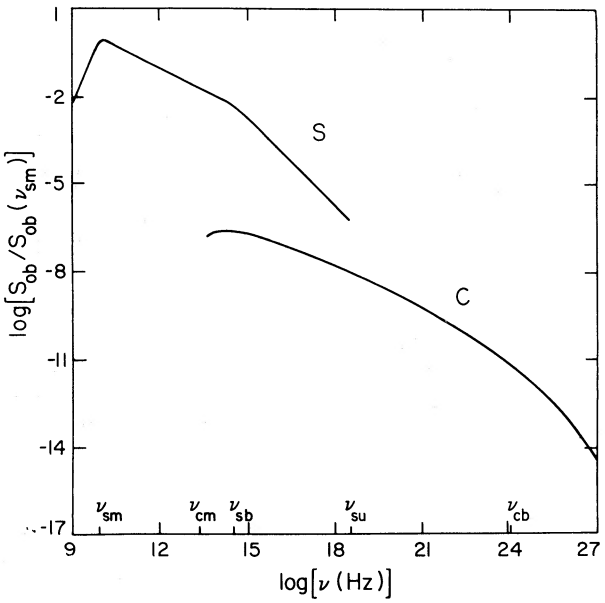

FIG. 1.—The local emission spectra in the jet. The model synchrotron spectrum (labeled *S*) has an injection spectral index $\alpha_0 = 0.5$. The once-scattered inverse-Compton spectrum (labeled *C*) was calculated for this model spectrum using equations (7) and (9). The spectra displayed in this figure represent the local emission spectra at a distance of 1 pc from the origin in the inhomogeneous-jet model described in the caption of Fig. 2. All the frequencies marked in the figure are defined in the text.

self-absorption, and the flux density rises as $\nu_s^{2.5}$. The optically thin spectrum has a spectral index $\alpha_s = \alpha_0$ between ν_{sm} and ν_{sb}, and $\alpha_s = \alpha_0 + 0.5$ between ν_{sb} and ν_{su}, where ν_{sb} and ν_{su} are the characteristic emission frequencies of electrons with Lorentz factors γ_{eb} and γ_{eu}, respectively. Above ν_{su} the flux density falls off exponentially with frequency. The frequency $\nu_{sm}(r)$ is approximated by setting the optical depth to synchrotron self-absorption equal to unity. Assuming that $B = B_1 r^{-m}$ and $K = K_1 r^{-n}$ (where cgs units apply to every quantity except r, which is expressed in parsecs), one obtains

$$\nu_{sm}(r) \approx (1+z)^{-1}[6.2 \times 10^{18} C_2(\alpha_0) \mathscr{D}_j^{1.5+\alpha_0} K_1 B_1^{1.5+\alpha_0} \varphi \csc\theta]^{1/(2.5+\alpha_0)} r^{-k_m} \text{ Hz}, \quad (3)$$

where $C_2(\alpha_0)$ is a constant (e.g., Blumenthal and Gould 1970; $C_2(0.5) = 8.4 \times 10^{10}$ cgs), and where $k_m = [(3+2\alpha_0)m + 2n - 2]/(5+2\alpha_0)$. (All the labeled k-coefficients defined in this paper are assumed to be positive numbers.) The observed size of the optically thick "core" of the jet thus varies with frequency as ν_s^{-1/k_m}. The frequency $\nu_{sb}(r)$ is estimated by equating the jet travel time to a distance r with the synchrotron cooling time (cf. Paper I). This gives

$$\nu_{sb}(r) \approx 6.9 \times 10^7 (1+z)^{-1} \mathscr{D}_j \gamma_j^2 \beta_j^2 B_1^{-3} r^{k_b} \text{ Hz}, \quad (4)$$

where $k_b = (3m-2)$. It will be assumed, for simplicity, that the values of γ_{el} and γ_{eu} are independent of r. (Note, however, that the discharge of relativistic electrons will be conserved along the jet only if the number density $n_e \approx K\gamma_{el}^{-2\alpha_0}/2\alpha_0$ scales as r^{-2}.) This assumption will be consistent with the requirements $\nu_{sm}(r)/\nu_{sb}(r) > \gamma_{el}^2/\gamma_{eb}^2$ and $\nu_{su}(r) = 10^6(1+z)^{-1}\mathscr{D}_j B_1 \gamma_{eu}^2 r^{-m} > \nu_{sb}(r)$ as long as r is not too large. The smallest radius from which optically thin emission with $\alpha_s = \alpha_0$ is observed can be determined by setting $\nu_{sb}(r) = \nu_{sm}(r)$ and is given, for $\alpha_0 = 0.5$, by

$$r_M \approx [1.6 \times 10^6 \mathscr{D}_j^{-1} (\gamma_j \beta_j)^{-6} K_1 B_1^{11} \varphi \csc\theta]^{1/(11m+n-7)} \text{ pc}. \quad (5)$$

The frequency $\nu_{sm}(r_M) \equiv \nu_{sM}$ is given, for $\alpha_0 = 0.5$, by

$$\nu_{sM} \approx 6.9 \times 10^7 (1+z)^{-1} [(1.6 \times 10^6 K_1 \varphi \csc\theta)^{3m-2} \mathscr{D}_j^{8m+n-5} (\gamma_j\beta_j)^{4m+2n-2} B_1^{-(3n+1)}]^{1/(11m+n-7)} \text{ Hz}. \quad (6)$$

The emissivity ϵ_c due to a single inverse-Compton scattering of synchrotron photons (with spectral index α_s) by relativistic electrons (with emission spectral index α_e) can be estimated using the δ-function approximation (e.g., Rieke and Weekes 1969). According to this approximation, the final frequency of a scattered photon is given by $\nu_c' \approx \gamma_e^2 \nu_s'$ and $\nu_c' \approx \gamma_e m_e c^2$ for $\gamma_e h\nu_s' \le m_e c^2$ (the Thomson regime) and $\gamma_e h\nu_s' > m_e c^2$ (the Klein-Nishina regime), respectively, where ν_s' is the initial frequency of the photon, γ_e is the Lorentz factor of the scattering electron, m_e is the electron's rest mass, and h is Planck's constant. The emissivity ϵ_c^T due to scattering with the Thomson cross section σ_T is then given by

$$\epsilon_c^T[(1+z)\nu_c/\mathscr{D}_j] \approx K_e \sigma_T r \varphi \epsilon_s [(1+z)\nu_c/\mathscr{D}_j] \int_{\gamma_{\min}}^{\gamma_{\max}} \gamma^{2(\alpha_s-\alpha_e)-1} d\gamma,$$

$$\gamma_{e\min}^2 \nu_{s\min} \le \nu_c \le \min\{\gamma_{e\max}^2 \nu_{s\max};\ \gamma_{e\max}\mathscr{D}_j m_e c^2/(1+z)h;\ [\mathscr{D}_j m_e c^2/(1+z)h]^2/\nu_{s\min}\}, \quad (7)$$

where

$$\gamma_{\min} = \max\{\gamma_{e\min};\ (\nu_c/\nu_{s\max})^{1/2};\ (1+z)h\nu_c/\mathscr{D}_j m_e c^2\},$$

$$\gamma_{\max} = \min\{\gamma_{e\max};\ (\nu_c/\nu_{s\min})^{1/2}\}, \quad (8)$$

and where the appropriate values of α_s, α_e, K_e, $\gamma_{e\min}$, $\gamma_{e\max}$, $\nu_{s\min}$, and $\nu_{s\max}$ are summarized in Table 1. The emissivity ϵ_c^{KN} due to scattering with the Klein-Nishina cross section is given in this approximation by

$$\epsilon_c^{KN}[(1+z)\nu_c/\mathscr{D}_j] \approx \tfrac{3}{8} K_e \sigma_T r \varphi \epsilon_s [(1+z)\nu_c/\mathscr{D}_j][\mathscr{D}_j m_e c^2/(1+z)h]^{2(\alpha_e+1)} \nu_c^{\alpha_s - 2\alpha_e - 1}$$
$$\times \left(\frac{\nu^{-(\alpha_s+1)}}{\alpha_s+1} \left[\frac{\alpha_s+3}{2(\alpha_s+1)} + \ln \left| \left[\frac{(1+z)h}{\mathscr{D}_j m_e c^2} \right]^2 2\nu\nu_c \right| \right] \right)_{\nu_{\max}}^{\nu_{\min}},$$

$$\max\{\mathscr{D}_j \gamma_{e\min} m_e c^2/(1+z)h;\ [\mathscr{D}_j m_e c^2/(1+z)h]^2/\nu_{s\max}\} \le \nu_c \le \mathscr{D}_j \gamma_{e\max} m_e c^2/(1+z)h, \quad (9)$$

where $\nu_{\min} = \max\{\nu_{s\min}; [\mathscr{D}_j m_e c^2/(1+z)h]^2/\nu_c\}$ and $\nu_{\max} = \nu_{s\max}$. The total inverse-Compton emissivity, $\epsilon_c = \epsilon_c^T + \epsilon_c^{KN}$, is generally dominated by ϵ_c^T in the scattered-photon frequency range where the Thomson regime and the Klein-Nishina regime overlap. (Note that the Klein-Nishina frequency range, given in eq. [9], is contained entirely in the Thomson frequency range, given in eq. [7], when $\gamma_{e\max} h\nu_{s\min}' < m_e c^2$.) The δ-function approximation yields an overestimate of the

TABLE 1

LOCAL RELATIVISTIC ELECTRON DISTRIBUTION AND OPTICALLY THIN SYNCHROTRON SPECTRUM IN THE JET

K_e	α_e	$\gamma_{e\min}$	$\gamma_{e\max}$	ϵ_s	α_s	$\nu_{s\min}$	$\nu_{s\max}$
K	α_0	γ_{el}	γ_{eb}	const. $\nu_s^{-\alpha_0}$	α_0	ν_{sm}	ν_{sb}
$K\gamma_{eb}$	$\alpha_0 + 0.5$	γ_{eb}	γ_{eu}	const. $(\nu_s/\nu_{sb})^{-0.5}\nu_s^{-\alpha_0}$	$\alpha_0 + 0.5$	ν_{sb}	ν_{su}

true emissivity, since the scattered photons are given roughly the maximum possible energy. For example, in the limit $\gamma_{e\,\min}{}^2\nu_{s\,\max} \leq \nu_c \leq \gamma_{e\,\max}{}^2\nu_{s\,\min}$, equation (7) overestimates the correct emissivity (e.g., Blumenthal and Gould 1970) by a factor $\lesssim 2$ (for $0 \leq \alpha_e \leq 1$). This approximation, however, is sufficiently accurate for the applications discussed in this paper.

The once-scattered synchrotron self-Compton spectrum corresponding to the optically thin portion of the model synchrotron spectrum is illustrated in Figure 1. (The inverse-Compton emission associated with the optically thick portion of the synchrotron spectrum is relatively small and can be neglected.) The spectrum extends between the frequencies $\nu_{cm} \equiv \gamma_{el}{}^2\nu_{sm}$ and min $\{\nu_{cu}; \nu_{KN}\}$, where $\nu_{cu} \equiv \gamma_{eu}{}^2\nu_{su}$ and $\nu_{KN} \equiv \gamma_{eu}\mathscr{D}_j m_e c^2/(1+z)h$. It essentially reproduces the shape of the optically thin synchrotron spectrum, with a break occurring near $\nu_{cb} \equiv \gamma_{eb}{}^2\nu_{sb}$ [$\gamma_{eb}{}^2 \approx 10^{-6}(1+z)\mathscr{D}_j{}^{-1}B^{-1}\nu_{sb}$], where the spectral index changes from $\alpha_c \approx \alpha_0$ to $_1\alpha_c \approx \alpha_0 + 0.5$. The spectra corresponding to higher-order inverse-Compton scatterings of the synchrotron photons can be calculated in an analogous way and have similar shapes.

The quasi-steady flux in the jet can vary as a result of fluctuations in the energy source at the origin. The time scale for flux decay in any given outburst cannot, however, be shorter than the radiative cooling time of the relativistic electrons which produce the observed emission. The electron cooling time is given by

$$t_{\rm cool} \approx 3 \times 10^7(1+z)\mathscr{D}_j{}^{-1}\gamma_e{}^{-1}[(1+\eta_c)B^2/8\pi]^{-1}\ \text{s}\ , \tag{10}$$

where

$$\eta_c \approx (K_e\sigma_{\rm T}r\varphi)\int_{\gamma_{e\,\min}}^{\gamma_{e\,\max}} \gamma_e{}^{1-2\alpha_e}d\gamma_e$$

is the ratio of the Compton-scattered photon energy density to the synchrotron energy density. Since the source is assumed to be synchrotron-loss dominated ($\eta_c \ll 1$), $t_{\rm cool}$ is essentially the synchrotron cooling time. For synchrotron radiation observed at a frequency ν_s, $\gamma_e{}^{-1} \approx 10^3(1+z)^{-1/2}\mathscr{D}_j{}^{1/2}B^{1/2}\nu_s{}^{-1/2}$. For Thomson-scattered synchrotron radiation observed at a frequency ν_c, a lower limit on $t_{\rm cool}$ is obtained by substituting $\nu_s{}^{-1/2} \approx \nu_c{}^{-1/2}\gamma_{\rm min}$ (cf. eq. [8]) in the expression for $\gamma_e{}^{-1}$. The cooling time scale generally increases with radius.

The above expressions are used in § II*b* to derive a model spectrum for an unresolved nonuniform jet. However, they are also useful for an analysis of the observed spectrum from a homogeneous emission region, as is illustrated in § III*c*.

b) Spectrum of an Unresolved Jet

The observed optically thin flux density $S_{\rm ob}(\nu)$ emitted between $r_{\rm min}$ and $r_{\rm max}$ from an unresolved conical jet is given by

$$S_{\rm ob}(\nu) = [(1+z)\mathscr{D}_j{}^2/4\pi D_l{}^2]\int_{r_{\rm min}}^{r_{\rm max}} \epsilon[(1+z)\nu/\mathscr{D}_j]\pi(r\varphi)^2 dr\ , \tag{11}$$

where $D_l = 10^9 D_{l9}$ pc is the luminosity distance to the source. Equation (11) is now used to calculate the synchrotron and inverse-Compton spectra for an inhomogeneous jet extending between r_l and r_u ($r_l \ll r_u$), with ϵ, $r_{\rm min}$, and $r_{\rm max}$ determined on the basis of the model presented in § II*a*.

Consider first the synchrotron spectrum, for which the emissivity is given by equation (2). In the frequency range $\nu_{sm}(r_u) \lesssim \nu_s \leq \nu_{sM}$, where ν_{sM} is given by equation (6), the observed flux density at ν_s is dominated by emission from $r_{\rm min}(\nu_s) = (\nu_s/\nu_{sM})^{-1/k_m}r_M$, obtained from equation (3) by setting $\nu_{sm}(r) = \nu_s$ and substituting for r_M from equation (5). Note that $r_{\rm min}(\nu_s)$ decreases to r_M as ν_s increases to ν_{sM}. For frequencies in the range $\nu_{sM} \leq \nu_s \lesssim \nu_{sb}(r_u)$, the flux density is dominated by emission from $r_{\rm min}(\nu_s) = (\nu_s/\nu_{sM})^{1/k_b}r_M$, which is obtained by setting $\nu_{sb}(r) = \nu_s$ in equation (4), and which now increases with frequency. In both of these cases $r_{\rm max} = r_u$, and so equation (11) gives

$$S_{\rm ob\,}{}_s(\nu_s) = \begin{cases} S_{\rm ob\,}{}_s(\nu_{sM})(\nu_s/\nu_{sM})^{-\alpha_{s1}} & \nu_{sM}(r_u/r_M)^{-k_m} \lesssim \nu_s \leq \nu_{sM}\ , \\ S_{\rm ob\,}{}_s(\nu_{sM})(\nu_s/\nu_{sM})^{-\alpha_{s2}} & \nu_{sM} \leq \nu_s \lesssim \nu_{sM}(r_u/r_M)^{k_b}\ , \end{cases} \tag{12}$$

where, setting

$$k_s = (1+\alpha_0)m + n - 3\ ,$$

$$S_{\rm ob\,}{}_s(\nu_{sM}) \approx 3 \times 10^4[C_1(\alpha_0)/C_1(0.5)](1+z)^{1-\alpha_0}D_{l9}{}^{-2}\mathscr{D}_j{}^{2+\alpha_0}\varphi^2 K_1 B_1{}^{1+\alpha_0}\nu_{sM}{}^{-\alpha_0}r_M{}^{-k_s}/k_s\ \text{Jy}\ ,$$

and where $\alpha_{s1} = (4+m-5k_m)/2k_m$ and $\alpha_{s2} = \alpha_0 + k_s/k_b$. [It is assumed here that $r_M \geq r_l$; if $r_l \gg r_M$, then the spectrum between $\nu_{sm}(r_l)$ and $\nu_{sb}(r_l)$ is dominated by emission with spectral index α_0 from r_l. In addition, it is assumed that $k_s/k_b < 0.5$; if $k_s/k_b \geq 0.5$, then the spectrum above ν_{sM} is dominated by emission with spectral index $(\alpha_0 + 0.5)$ from r_M.] The spectral indices α_{s1} and α_{s2} represent the effect of the nonuniformity of the source in the optically thick and optically thin regimes, respectively. (The flattening of the optically thick spectrum in an inhomogeneous synchrotron source has previously been pointed out by Condon and Dressel [1973], de Bruyn [1976], and Marscher [1977]. The steepening of the optically thin spectrum in such a source was considered by Marscher [1980], who, however, assumed no reacceleration of the injected relativistic electrons.) For frequencies in the range $\nu_{sb}(r_u) \lesssim \nu_s \lesssim \nu_{su}(r_u)$, the spectrum is dominated by

emission from near r_u with spectral index $(\alpha_0 + 0.5)$, whereas above $\nu_{su}(r_u)$ the emission comes predominantly from $r_{\max}(\nu_s) = [\nu_s/\nu_{su}(r_u)]^{-1/m} r_u$, and the spectral index is approximately $\alpha_{s3} = (m + 2 - n)/m$. The synchrotron spectrum terminates near $\nu_{su}(r_u)$. This description is only approximate, and the actual spectrum changes slope continuously over a wide range of frequencies. An example of a synchrotron spectrum calculated in this way is shown in Figure 2. It is seen that the nonuniformity of B and K can give rise to an integrated spectrum which is quite different from the underlying emission spectrum (cf. Fig. 1). In turn, it should in principle be possible to deduce the values of m and n (as well as of α_0) from the observed shape of the spectrum. (Note that this cannot be done in models where only the optically thick spectrum is affected by the source inhomogeneity; cf. Marscher 1977.) For example, if $\alpha_0 = 0.5$ and $\alpha_{s1} = 0$, then $n = (17 - 7m)/5, \alpha_{s2} = (8m - 3)/(15m - 10)$, and $\alpha_{s3} = (12m - 7)/5m$. If the magnetic field is converted by the jet, then, in a conical geometry, m can vary between 1 and 2 (e.g., Blandford and Rees 1974). Correspondingly, in this example, n, α_{s2}, and α_{s3} lie in the ranges 2–0.6, 1–0.65, and 1–1.7, respectively, and for $m = 1$, the magnetic and electron energy densities are in equipartition (this special case was considered in Paper I).

The synchrotron self-Compton spectrum is calculated on the assumption that the emission at radius r is mainly due to the scattering of photons produced within a distance $\sim (r\varphi)$ from the scattering site. Even though the optical depth to Thomson scattering, $\tau_c \approx \mathscr{D}_j^{-1} \sigma_T K_e r\varphi \csc\theta \gamma_{e\,\min}^{-2\alpha_e/\alpha_e}$ (for a line of sight passing through the jet at a distance r from the apex), is typically $\ll 1$, this assumption is valid for a sufficiently narrow jet ($\varphi \ll 1$). In this case, equations (7) and (9) for the local emissivities are applicable. The once-scattered photon spectrum lies in the range $\nu_{cm}(r_u) \lesssim \nu_c \lesssim \min\{\nu_{cu}(r_M); \nu_{KN}\}$. In a manner similar to the synchrotron-spectrum calculation, one finds that the observed flux density just below $\nu_{cM} \equiv \nu_{cm}(r_M)$ is given by

$$S_{ob\,c}(\nu_c) = S_{ob\,c}(\nu_{cM})(\nu_c/\nu_{cM})^{-\alpha_{c1}}, \tag{13}$$

where, setting $k_c = k_s + n - 1$,

$$S_{ob\,c}(\nu_{cM}) \approx 0.03(k_m/k_c^2)[C_1(\alpha_0)/C_1(0.5)](1+z)^{1-\alpha_0} D_{l9}^{-2} \mathscr{D}_j^{2+\alpha_0} \varphi^3 K_1^2 B_1^{1+\alpha_0} \nu_{cM}^{-\alpha_0} r_M^{-k_c} \text{ Jy},$$

and where $\alpha_{c1} = \max\{-(k_c/k_m - \alpha_0); -1\}$. (An optically thin inverse-Compton spectrum cannot rise faster than $S_{ob\,c} \propto \nu_c$; e.g., Blumenthal and Gould 1970.) For $\nu_{cM} \lesssim \nu_c \lesssim \nu_{cb}(r_M)$, the spectrum is dominated by emission from near r_M with spectral index α_0, whereas for $\nu_{cb}(r_M) \lesssim \nu_c \lesssim \nu_{cb}(r_u)$, the spectral index is approximately $\alpha_{c2} = \alpha_0 + k_c/(2k_b + m)$. The spectral indices α_{c1} and α_{c2}, like α_{s1} and α_{s2} in the synchrotron spectrum, arise because of the inhomogeneity of the source. The once-scattered photon spectrum is also illustrated in Figure 2. The higher-order inverse-Compton spectra display similar behavior, but in the frequency range of interest they generally lie well below the once-scattered photon spectrum

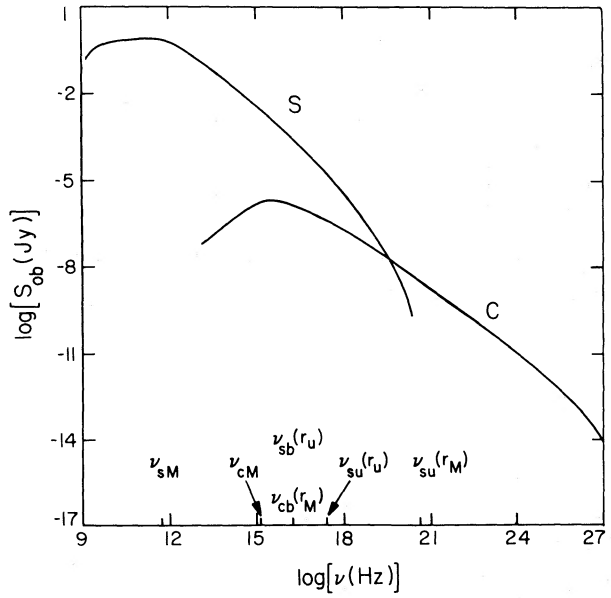

FIG. 2.—The synchrotron and inverse-Compton spectra for an unresolved inhomogeneous jet. This example corresponds to a relativistic conical jet with $D_{l9} = 0.5$, $\mathscr{D}_j = \gamma_j = \csc\theta = 5$, $\varphi = 0.1$, and a synchrotron spectrum with $\nu_{sm}(r_u) = 10^9$ Hz, $\nu_{sM} = 5 \times 10^{11}$ Hz, $S_{ob\,s}(\nu_{sM}) = 1.0$ Jy, $\alpha_0 = 0.5$, $\alpha_{s1} = 0$, and $\alpha_{s2} = 0.8$. (All the quantities referred to in the legend or marked in the figure are defined in the text.) Using these observable parameters in eqs. (5), (6), and (12), one obtains $m = 1.25$, $n = 1.65$, $K_1 = 1.7 \times 10^2$ cm^{-3}, $B_1 = 2.9 \times 10^{-2}$ G, $r_M = 2.3 \times 10^{-2}$ pc, and $r_u/r_M = 3.7 \times 10^2$. These values, as well as $\gamma_{el} = 50$ and $\gamma_{eu} = 5 \times 10^6$, were used in eqs. (2), (7), (9), and (11) to generate the synchrotron spectrum (labeled S) and the once-scattered inverse-Compton spectrum (labeled C) which are shown here. Note that in this example $\alpha_{s3} = 1.28$, $\alpha_{c1} = 0.62$, and $\alpha_{c2} = 0.75$. The local emission spectra in this jet at a distance of 1 pc from the origin are displayed in Fig. 1.

for typical radio-jet parameters. For example, the maximum observed flux density of the twice-scattered photon spectrum is given approximately by

$$S_{\mathrm{ob}\,cc}(\nu_{ccM}) \approx 3 \times 10^{-8}(k_m{}^2/k_{cc}{}^3)[C_1(\alpha_0)/C_1(0.5)](1+z)^{1-\alpha_0} \times |D_{19}{}^{-2}\mathscr{D}_j{}^{2+\alpha_0}\varphi^4 K_1{}^3 B_1{}^{1+\alpha_0}\nu_{ccM}{}^{-\alpha_0} r_M{}^{-k_{cc}}\ \mathrm{Jy}\ , \quad (14)$$

where $\nu_{ccM} \equiv \gamma_{el}{}^4 \nu_{sm}$ and $k_{cc} = k_c + n - 1$, which may be compared with the analogous expression for the once-scattered photon flux given by equation (13).

The inverse-Compton spectrum steepens once the Klein-Nishina regime is reached (cf. Fig. 2). The high-energy flux could in principle be attenuated also by collisions between once-scattered synchrotron photons of frequencies $\nu_c \gtrsim (2)^{1/2}\mathscr{D}_j m_e c^2/(1+z)h$ and synchrotron photons of frequencies $\nu_s \approx 2[\mathscr{D}_j m_e c^2/(1+z)h]^2/\nu_c$, which produce e^+e^- pairs with cross section $\sigma_p \approx 10^{-25}$ cm^2 (e.g., Jelley 1966). However, the optical depth for this process, $\tau_p(\nu_c) \approx \mathscr{D}_j{}^{-1}\{\epsilon_s[2\mathscr{D}_j(m_e c^2/h)^2/(1+z)\nu_c]r\varphi/hc\}\sigma_p\{2r\varphi \csc\theta\}$, evaluated at $r_{\min}(\nu_c)$, is typically much smaller than unity, so in practice the attenuation is negligible. Recall that in this model most of the energy emitted from the jet is assumed to be synchrotron radiation (see the discussion following eq. [10]). If the integrated synchrotron spectrum breaks near $\nu_s{}^*$ from $\alpha_s < 1$ to $\alpha_s > 1$, then most of the energy is emitted near $\nu_s{}^*$. The precise value of $\nu_s{}^*$ depends of course on the parameters of the source, but note that for $\alpha_{s2} < 1 < \alpha_0 + 0.5$, it lies in the frequency range dominated by emission from the outer region of the jet.

The spectra displayed in Figure 2 are calculated for a representative beamed source. It is assumed in this calculation that $\mathscr{D}_j \approx \gamma_j \approx \csc\theta$, which for a source observed at a given angle θ is the combination which maximizes the Doppler factor $\mathscr{D}_j$. (In this case the apparent velocity β_{ob} is also $\sim \mathscr{D}_j$; cf. Paper I.) Those portions of the spectrum which arise essentially in the same region (e.g., near r_M or r_u) should show correlated variability and could vary on a different time scale than the flux which is emitted from a different region (cf. eq. [10]). Although some of the specific assumptions used in calculating the spectrum, such as constant φ and β_j, may not all apply in real sources, this model can nevertheless be used to account for various broad features of observed spectra, as is discussed in the next section.

III. APPLICATIONS

a) Spectra of BL Lacertae Objects

BL Lac objects have been interpreted as extreme cases of beamed sources, in which the Doppler boost is so large that a substantial portion of the observed optical spectrum is dominated by the nonthermal contribution from the jet (see Blandford and Rees 1978*b* and Paper I). It is proposed here that the beamed component may in fact dominate most of the observed spectrum from radio frequencies through X-rays. In support of this hypothesis, it is shown that the model spectrum calculated in § II*b* for an unresolved, inhomogeneous relativistic jet could account for various properties of the spectra measured in these sources. First, general features are outlined for the different spectral regimes, and then a particular source (Mrk 421) is discussed in greater detail.

i) *Radio.* The radio spectra typically are flat and become optically thin near or above $\sim 10^{11}$ Hz, which is higher than the average break frequency for flat-radio-spectrum QSOs (e.g., Condon 1978). The spectra may be interpreted in the inhomogeneous-jet model as corresponding to $\alpha_{s1} \approx 0$, and the higher break frequency is consistent, by equation (6) for ν_{sM}, with a higher degree of beaming (i.e., with a larger value of $\mathscr{D}_j$ or of $\csc\theta$).

ii) *Optical.* The high degree of variability and strong linear polarization displayed by BL Lac objects may be associated with the beamed emission from the jet, as discussed in Paper I. However, the optical spectrum of some sources, such as Mrk 421 and Mrk 501 (e.g., Ulrich *et al.* 1975; Maza, Martin, and Angel 1978), appears to contain also a contribution from the associated elliptical galaxy and therefore cannot be compared with the model of § II*b*.

iii) *X-rays.* BL Lac objects have now been established also as a class of X-ray sources (e.g., Schwartz *et al.* 1979; Ku 1980). Present data indicate that below ~ 5 keV their spectra are generally soft ($\alpha \gtrsim 1$), but some sources, e.g., the Markarian galaxies 421 and 501 (Mushotzky *et al.* 1978*b*), and PKS 0548-322 (Riegler, Agrawal, and Mushotzky 1979), display a hard ($\alpha < 0.5$) component at higher energies. These two components could be interpreted as synchrotron radiation and once-scattered inverse-Compton radiation, respectively (cf. Margon, Jones, and Wardle 1978; Schwartz *et al.* 1978). In those sources where it was detected, the hard X-ray component has a flux density which is a fraction, (a few) times 10^{-6}, of the flat-spectrum radio flux density. This is consistent with the estimates of § II*b* for a reasonable choice of parameters in equations (5), (6), (12), and (13) and suggests that the absence of a detectable hard X-ray component in sources like PKS 2155-304 (e.g., Griffiths *et al.* 1979) is due to the fact that they have a relatively high ($\gtrsim 10^{-5}$) ratio of X-ray to radio flux densities at the observed X-ray frequencies. In the present model it is predicted that all sources would display a hard X-ray component at sufficiently high energies, that this component would on the average show less linear polarization than the soft X-ray component (reflecting the difference between the emission mechanisms attributed to these components), and that it would vary in correlation with the high-frequency ($\nu_s \lesssim \nu_{sM}$) radio flux density (since the bulk of the emission in both cases is assumed to come from the same region near r_M).

iv) *γ-rays.* No BL Lac object has as yet been detected in high-energy γ-rays, but upper limits set by Bignami *et al.* (1979) for Mrk 421 and Mrk 501 indicate that the flux density must decrease by a factor $> 10^2$ between 10 keV and 100 MeV. This means that the effective spectral index in this range exceeds 0.5, which is consistent with the behavior of the

once-scattered photon spectrum in the present model, and implies that the hard X-ray component measured in these sources in the 2–30 keV range (e.g., Mushotzky *et al.* 1978*b*) must steepen at higher energies.

As a specific application of the model, consider the source Mrk 421. The high degree of variability measured in this object, particularly in the optical and X-ray regimes, supports an association with a relativistic beamed source. However, because of the inherent variability and the incomplete spectral coverage, a steady state spectrum which could be compared with the model spectrum of § II*b* is still not well established. The observed radio spectrum is flat and shows no break below 90 GHz (cf. O'Dell *et al.* 1978) and so could conceivably join with the far-infrared spectrum, which is nonthermal with spectral index $\gtrsim 0.8$ (e.g., Ulrich *et al.* 1975; Maza, Martin, and Angel 1978). The UV spectrum measured by the *IUE* (Boksenberg *et al.* 1978) and the soft X-ray spectrum measured by Hearn, Marshall, and Jernigan (1979) below 6 keV have similar spectral indices (~ 1) and may in fact join together. The hard X-ray component measured by Mushotzky *et al.* (1978*b*) at higher energies was not detected at a later measurement (Mushotzky *et al.* 1979), which also revealed a steepening of the soft component. It is possible to give a self-consistent interpretation of these observations in the inhomogeneous-jet model. The measured spectrum from the radio to soft X-rays, excluding the galactic optical contribution, may be modeled by a synchrotron spectrum with $\alpha_{s1} \approx 0$, $\alpha_{s2} \approx 0.8$, and $\alpha_0 \approx 0.5$, and with the break frequencies ν_{sM}, $\nu_{sb}(r_u)$, and $\nu_{su}(r_u)$ being roughly 10^{12} Hz, 10^{15} Hz, and 10^{17} Hz, respectively. The soft X-ray component is then produced in the outer region of the jet near r_u, whereas the hard X-ray component, interpreted as once-scattered inverse-Compton emission, is produced in the inner region near r_M. It is therefore expected that the hard component would show a higher degree of variability, and the reported time scale of $\lesssim 1$ yr is consistent with the cooling-time estimate of equation (10). Mrk 421 also displayed a strong X-ray outburst on a time scale of ~ 10 days (Ricketts, Cooke, and Pounds 1976), for which no direct evidence exists at optical wavelengths, but which was observed in the radio, with amplitude that increased with frequency and a variability time scale of a few months (Margon, Jones, and Wardle 1978). If the outburst corresponded to a disturbance in the steady state conditions which propagated outward from the origin of the jet, then these observations are consistent with the radio emission coming from progressively smaller radii as the frequency of observation is increased toward ν_{sM} and with the optical radiation being emitted at $r \gg r_M$. Alternatively, the outburst could be interpreted as emission from clouds or shock waves traveling in the jet, which at lower radio frequencies would be obscured by the optically thick "core" of the jet (cf. Paper I).

b) Spectrum of 3C 273

The archetypal quasar 3C 273 has been observed at frequencies ranging from radio to high-energy γ-rays. It is associated with a core-jet radio source which is resolved by VLBI on a milli-arcsec scale (e.g., Readhead *et al.* 1979) and which shows evidence for relativistic motion in the form of apparent superluminal separation of radio components with $\beta_{ob} \approx 5.2$ (e.g., Cohen *et al.* 1979). The radio spectrum is flat and polarized (e.g., Rudnick *et al.* 1978) and could be accounted for by the inhomogeneous-jet model of § II*b*, which is compatible with the observed morphology of the source. The absence of an observed counterjet may be another indication that the radio source is beamed (e.g., Readhead *et al.* 1978).

The radio spectrum breaks at ~ 50 GHz and could conceivably be extrapolated to the infrared regime with $\alpha \approx 0.8$ (cf. Elias *et al.* 1978); however, the infrared component is much steeper and, like the optical component, shows little variability (e.g., Neugebauer *et al.* 1979) and low polarization (e.g., Kemp *et al.* 1977). These components thus appear to be distinct from the radio component, a conclusion which is supported by the apparent lack of correlation between the infrared-optical and the radio regimes in quasars in general (cf. Neugebauer *et al.* 1979). The observed UV flux (e.g., Boksenberg *et al.* 1978) is consistent with the ionizing continuum required to produce the unbeamed Hβ flux (e.g., Weedman 1976) and is probably also not associated with the jet.

X-ray spectral measurements of 3C 273 have been obtained by Primini *et al.* (1979) and by Worrall *et al.* (1979). The best-fit spectral index is ~ 0.4 in the range 2–60 keV and ~ 0.7 in the range 13–120 keV, with a change of slope indicated above ~ 20 keV. The X-ray flux appears to vary by a factor $\lesssim 2$ on a time scale of months. Both the spectral shape and the degree of variability are similar to those of Seyfert 1 galaxies (e.g., Mushotzky *et al.* 1980), which are generally weak radio sources and do not show evidence for beaming (e.g., Weedman 1977). A similarity with Seyfert 1 spectra is indicated also by X-ray measurements of other quasars (e.g., Apparao *et al.* 1978), but more observations are required to determine whether it holds for quasars in general. The X-rays could in principle also be once-scattered synchrotron self-Compton photons from the jet (cf. Jones 1979). However, it is difficult to fit the observed X-rays with the model spectrum of § II*b*, given the constraints imposed by the radio spectrum and by the apparent velocity.

As was mentioned in § I, 3C 273 is as yet the only quasar identified as a high-energy γ-ray source, with a possibly variable flux density of $\sim 2 \times 10^{-9}$ Jy around 100 MeV (Swanenburg *et al.* 1978). The γ-ray flux density is consistent with an extrapolation of the synchrotron spectrum with $\alpha \approx 1$ from the radio break frequency. (This spectrum would pass also through the observed X-ray regime, but is too steep to account for the observed X-ray spectrum.) However, the electron Lorentz factors required to produce such high-energy synchrotron emission must exceed 10^8. If the synchrotron spectral index above the break frequency is in fact smaller (~ 0.7–0.8), then it is also possible to interpret the γ-rays as once-scattered inverse-Compton radiation from the jet. For example, if $\alpha_0 = 0.5$, the once-scattered spectrum would steepen near $\nu_{cb}(r_M) \approx 10^{15}$–$10^{16}$ Hz, where $S_{obc} \approx 10^{-6}$ to 10^{-5} Jy, from $\alpha_c \approx 0.5$ to $\alpha_c \approx 0.6$–0.7, and could extend up to

the γ-ray region, passing below the observed X-ray spectrum. (Note that in the model of Jones [1979], the γ-rays are interpreted as *twice*-scattered synchrotron photons.)

To summarize, the radio emission in 3C 273 is attributed to an inhomogeneous relativistic jet which could also produce the high-energy γ-rays, but other parts of the observed spectrum appear to be unbeamed. It is therefore likely that the Doppler factor associated with the beamed component is relatively small, implying that the angle θ between the jet axis and the observer direction is relatively large. However, the high apparent velocity constrains θ to be less than or equal to $2\ \mathrm{ctn}^{-1}(\beta_{ob}) \approx 22°$ and indicates a large β_j. The origin of the γ-ray flux in 3C 273 is discussed further in § IV.

c) *X-Ray Emission from Resolved Jets*

The inhomogeneous-jet spectrum calculated in § II*b* is based on a simple synchrotron spectrum, as described in § II*a*. It is of interest to verify that the assumed local emission spectrum is in fact an adequate representation of the spectra observed in resolved jets. One suitable example is provided by the spectrum of emission knot A in the jet of M87 (e.g., Turland 1975; Redman 1978). The spectrum extends from $\sim 10^8$ Hz with $\alpha \approx 0.5$ and steepens above $\sim 10^{14}$ Hz to $\alpha \approx 1.3$. The recently discovered X-ray emission from this knot (e.g., Schreier *et al.* 1979*b*) is consistent with a linear extrapolation of this spectrum. The break at optical frequencies may be interpreted as due to synchrotron-radiation losses. (An increase in the spectral index by more than 0.5 could indicate that the reacceleration of relativistic electrons is not continuous; see Kellermann 1966.) It is then possible to estimate the magnetic field as a function of the size of the emission region and the velocity of the radiating material (cf. eq. [4]). This was done for knot A by Blandford and Königl (1979*a*), who interpreted the emission as radiation from behind a shock wave associated with a dense cloud which is accelerated by the jet (see also Rees 1978).

X-ray emitting knots have also been detected in Cen A, where they lie within the inner NE radio lobe and are aligned with the inner optical jet (e.g., Schreier *et al.* 1979*a*; Feigelson 1980). A large knot located about 1′ from the nucleus was measured by the *Einstein* HRI to have a diameter $d \approx 15''$ (≈ 0.4 kpc at a distance of 5 Mpc) and a surface brightness of $\sim 10^{-10}$ Jy arcsec^{-2} at $\sim 10^{17}$ Hz. By analogy with knot A in M87, it is proposed here that the X-rays be interpreted as synchrotron radiation emitted above the break frequency and arising behind a strong shock wave which travels in the jet. (Note that Schreier *et al.* [1979*a*] interpreted the X-ray emission as thermal in origin.) Unlike the case of the jet in M87, there is direct evidence in Cen A for radial motion of optical knots away from the nucleus (Osmer 1978; Dufour and van den Bergh 1978). The measured radial velocities are in the range $2.5\text{–}3.5 \times 10^7$ cm s^{-1} for knots lying at projected distances of 13–24 kpc from the nucleus. The relative uniformity of the velocity values supports the interpretation of the knots as clouds that have been accelerated by the jet. Furthermore, the spectrum of at least one of the optical knots may indicate excitation by a shock. The spectral break frequency ν_{sb} in the large X-ray knot can be estimated by adopting the equipartition value B_{eq} for the magnetic field in the emission region. Using an injection spectral index $\alpha = 0.65$ (which is compatible with the spectral indices of both the radio and the X-ray emission from the nucleus; cf. Mushotzky *et al.* 1978*a*) and a lower cutoff frequency of $\sim 10^8$ Hz, and writing the velocity of the jet as $v_j = 10^8 v_{j8}$ cm s^{-1} and the size of the knot as $d = 0.4 d_{0.4}$ kpc, one obtains $\nu_{sb} \approx 4 \times 10^8 {d_{0.4}}^{-2} {v_{j8}}^{7/2}$ Hz and $B_{eq} \approx 10^{-4} {v_{j8}}^{-1/2} G$. (Note that emission due to inverse-Compton scattering of the microwave background will not exceed the synchrotron emission as long as $B \gtrsim 3 \times 10^{-6} G$; e.g., Harris and Grindlay 1979.) Now, the X-ray knot is located within the radio ridge which appears in the 1.4 GHz ($\sim 1'$ resolution) map of Christiansen *et al.* (1977) between the nucleus and the inner NE lobe, but the map shows no enhanced radio emission at the position of the knot. In order not to exceed the radio surface brightness estimated from this map ($\sim 10^{-3}$ Jy arcsec^{-2}), the break frequency must be $> 10^{13}$ Hz (for $\alpha \approx 0.65$). This could be reconciled with the above estimate if either $d \ll 15''$ or $v_j \gg 10^8$ cm s^{-1}. The first possibility is consistent with the visual diameters of the moving knots measured by Osmer (1978), which are $\sim 1''$ (e.g., Blanco *et al.* 1975), especially in view of the fact that accelerated clouds would expand as they moved downstream in the jet (cf. Blandford and Königl 1979*a*). As regards the second possibility, it is conceivable that the velocity of the inner jet is actually much greater than the lower limit set by the radial velocities of the outer optical knots. If the jet velocity is even mildly relativistic, then, as in the case of M87 (e.g., Rees 1978), this could account for the absence of an observed counterjet. As was discussed by Blandford and Königl (1979*a*; Paper I), the knots could be either interstellar clouds (which may form in the inner optical jet of Cen A by a thermal instability; cf. Schreier *et al.* 1979*a*), planetary nebulae, or supernova remnants. They might also be portions of the jet's wall which were torn off near the origin of the jet by hydrodynamical instabilities. High-resolution radio observations and sensitive spectroscopic measurements should be able to determine the actual sizes of the X-ray emitting knots, their velocities, and their origin.

IV. DISCUSSION

As was mentioned in § I, recent X-ray observations suggest that a large fraction of quasars and BL Lac objects are also X-ray sources. Although the sample is still incomplete, there are indications that BL Lac objects and optically violently variable quasars have a higher ratio of X-ray to optical luminosity than radio-quiet QSOs (e.g., Ku and Helfand 1980). This is manifested in the value of the effective optical–to–X-ray spectral index α_{ox} (defined, e.g., by Tananbaum *et al.* 1979), which is ~ 1.25 for blazars and ~ 1.5 for radio-quiet QSOs. These spectral indices could be interpreted as corresponding, respectively, to the beamed and isotropic emission spectra in quasars. In fact, the deduced value of α_{ox} for blazars is consistent with the soft X-ray component measured in several BL Lac objects, as discussed in § III*a*.

Alternatively, the larger average X-ray luminosity in blazars could reflect an increase in the relative contribution of the beamed component in these sources on going from optical to X-ray frequencies. Ku and Helfand (1980) analyzed the statistical properties of a sample of active galactic nuclei and found a good correlation between the X-ray (2 keV) and optical (2500 Å) fluxes, but no correlation between the X-ray flux and the radio flux at 5 GHz. These properties are consistent with the X-rays being associated with the isotropic optical component rather than with the beamed radio emission (cf. § III*b*). However, these results are also consistent with the model spectrum for strongly beamed sources discussed in the previous sections, in which the soft X-ray component is a continuation of the optical component, but is distinct from the radio component. As was noted by Ku and Helfand (1980), the low-frequency radio emission could actually come from a steep-spectrum halo. This may well be the case for the beamed sources, in which the halo would correspond to an outer radio lobe seen head on (cf. Paper I).

It has been suggested, on the basis of their observed X-ray luminosities and apparently strong cosmological evolution, that quasars account for most of the diffuse X-ray background in the few keV range (e.g., Setti and Woltjer 1979; Tananbaum *et al.* 1979). However, Schwartz *et al.* (1978) estimated that, in the absence of density evolution, BL Lac objects contribute only a few percent of the background in that energy range. Of course, this estimate could be revised if BL Lac objects are shown to evolve, or if their volume emissivity is larger than that assumed by Schwartz *et al.* (1978). According to the beaming hypothesis, radio-loud QSOs (as a subset of optically selected QSOs) and BL Lac objects (as a subset of giant elliptical galaxies) are the intrinsically faint sources which are brightened by the relativistic Doppler effect. If the Lorentz factors associated with the beamed components in these two types of sources are comparable, then the fraction of radio-loud quasars among optically selected QSOs ($\lesssim 10\%$; e.g., Sramek and Weedman 1978) is expected to be of the same order as the fraction of BL Lac objects among giant elliptical galaxies. This is in fact consistent with the current space-density estimates of BL Lac objects ($\sim 10^2$ Gpc^{-3}; e.g., Setti 1978) and of giant elliptical galaxies ($\sim 10^4$ Gpc^{-3}; e.g., Schmidt 1966). However, at least some BL Lac objects appear to be associated with elliptical galaxies at the top of the luminosity function (e.g., Kinman 1978; Griffiths *et al.* 1979), suggesting that there may be many more faint BL Lac objects which have not yet been identified. Setti and Woltjer (1979) noted that if quasars account for much of the observed X-ray background, then only about 5% of them could have the same ratio of X-ray to γ-ray flux density as 3C 273 if the diffuse high-energy γ-ray background is not to be exceeded. If 3C 273 is a typical quasar, then this fact may have important consequences when interpreted in the context of the beaming hypothesis. It could suggest the existence of a correspondence between radio-loud and γ-ray loud quasars, implying that both the radio and the γ-ray emission in 3C 273 originate in the beamed jet. Such a correspondence would also imply that the diffuse background at high ($\gtrsim 100$ MeV) energies is dominated by radiation from beamed sources. Of course, these inferences are merely suggestive and could only be checked after additional extragalactic high-energy γ-ray sources are detected. Note that if the ratio of γ-ray to X-ray flux density in BL Lac objects is comparable to that in 3C 273, then Lacertids would contribute a substantial fraction of the diffuse γ-ray background even without evolution. If most of the high-energy background is produced by beamed sources with similar spectra, then the observed spectrum of the background at these energies (e.g., Fichtel, Simpson, and Thompson 1978) should reflect the shape of the individual spectra. In addition, improved limits on the isotropy of the background could constrain the number density of these sources (cf. Schwartz and Gursky 1974).

V. SUMMARY

This paper considered the radio–through–γ-ray emission from relativistic jets associated with bright, compact radio sources. A simple local synchrotron-emission spectrum was adopted, with an assumed break frequency determined by equating the synchrotron cooling time to the expansion time. This spectrum was applied to the interpretation of emission knots in the jets of M87 and of Cen A, and to the calculation of a synchrotron and inverse-Compton spectra for an unresolved inhomogeneous jet. In this calculation it was shown how the nonuniformity of the magnetic field and of the relativistic-electron density in the source could give rise to an integrated spectrum which is quite different from the local emission spectrum in both the optically thick and the optically thin regimes. It was pointed out which parts of the integrated spectrum are emitted from the same region of the jet, and would therefore be expected to show correlated variability. The inhomogeneous-jet model was applied to the interpretation of the spectra of BL Lac objects. In particular, it could account for the flat radio spectrum and the relatively high break frequency, as well as for the soft component and the more highly variable hard component observed in X-rays. On the basis of this model, it was predicted that a hard spectral component would be detected in all BL Lac objects at sufficiently high energies, that it would be less strongly polarized than the soft X-ray component, and that it would vary in correlation with the high-frequency radio emission. In the case of 3C 273, it was concluded that the infrared–through–X-ray spectrum is probably unbeamed, but that the radio flux and possibly also the high-energy γ-rays could be attributed to the relativistic inner radio jet. Finally, the distinguishing properties of blazars as a class of X-ray sources were considered in the context of the relativistic-jet model, and it was pointed out that beamed sources could contribute a major fraction of the diffuse high-energy γ-ray background.

I thank Roger Blandford and David Payne for valuable suggestions and encouragement.

REFERENCES

Angel, J. R. P., and Stockman, H. S. 1980, *Ann. Rev. Astr. Ap.*, **18**, 321.
Apparao, K. M. V., Bignami, G. F., Maraschi, L., Helmken, H., Margon, B., Hjellming, R., Bradt, H. V., and Dower, R. G. 1978, *Nature*, **273**, 450.
Bignami, G. F., Fichtel, C. E., Hartman, R. C., and Thompson, D. J. 1979, *Ap. J.*, **232**, 649.
Blanco, V. M., Graham, J. A., Lasker, B. M., and Osmer, P. S. 1975, *Ap. J. (Letters)*, **198**, L63.
Blandford, R. D., and Königl, A. 1979*a*, *Ap. Letters*, **20**, 15.
———. 1979*b*, *Ap. J.*, **232**, 34 (Paper I).
Blandford, R. D., and Rees, M. J. 1974, *M.N.R.A.S.*, **169**, 395.
———. 1978*a*, *Phys. Scripta*, **17**, 265.
———. 1978*b*, in *Pittsburgh Conference on BL Lac Objects*, ed. A. M. Wolfe (Pittsburgh: University of Pittsburgh), p. 328.
Blumenthal, G. R., and Gould, R. J. 1970, *Rev. Mod. Phys.*, **42**, 237.
Boksenberg, A., *et al.* 1978, *Nature*, **275**, 404.
Christiansen, W. N., Frater, R. H., Watkinson, A., O'Sullivan, J. D., and Lockhart, I. A. 1977, *M.N.R.A.S.*, **181**, 183.
Cohen, M. H., Pearson, T. J., Readhead, A. C. S., Seielstad, G. A., Simon, R. S., and Walker, R. C. 1979, *Ap. J.*, **231**, 293.
Condon, J. J. 1978, in *Pittsburgh Conference on BL Lac Objects*, ed. A. M. Wolfe (Pittsburgh: University of Pittsburgh), p. 21.
Condon, J. J., and Dressel, L. L. 1973, *Ap. Letters*, **15**, 203.
de Bruyn, A. G. 1976, *Astr. Ap.*, **52**, 439.
Dufour, R. J., and van den Bergh, S. 1978, *Ap. J. (Letters)*, **226**, L73.
Elias, J. H., *et al.* 1978, *Ap. J.*, **220**, 25.
Feigelson, E. 1980, Ph.D. thesis, Harvard University.
Fichtel, C. E., Simpson, G. A., and Thompson, D. J. 1978, *Ap. J.*, **222**, 833.
Griffiths, R. E., Tapia, S., Briel, V., and Chaisson, L. 1979, *Ap. J.*, **234**, 810.
Harris, D. E., and Grindlay, J. E. 1979, *M.N.R.A.S.*, **188**, 25.
Hearn, D. R., Marshall, F. J., and Jernigan, J. G. 1979, *Ap. J. (Letters)*, **227**, L63.
Jelley, J. V. 1966, *Nature*, **211**, 472.
Jones, T. W. 1979, *Ap. J.*, **233**, 796.
Kellermann, K. I. 1966, *Ap. J.*, **146**, 621.
Kemp, J. C., Rieke, G. H., Lebofsky, M. J., and Coyne, G. V. 1977, *Ap. J. (Letters)*, **215**, L107.
Kinman, T. D. 1978, in *Pittsburgh Conference on BL Lac Objects*, ed. A. M. Wolfe (Pittsburgh: University of Pittsburgh), p. 82.
Ku, W. H. M. 1980, *Highlights in Astronomy*, in press.
Ku, W. H. M., and Helfand, D. J. 1980, Columbia Ap. Lab. Contr. No. 186.
Margon, B., Jones, T. W., and Wardle, J. F. C. 1978, *A.J.*, **83**, 1021.
Marscher, A. P. 1977, *Ap. J.*, **216**, 244.
———. 1980, *Ap. J.*, **235**, 386.
Maza, J., Martin, P. G., and Angel, J. R. P. 1978, *Ap. J.*, **224**, 368.
Mushotzky, R. F., Boldt, E. A., Holt, S. S., Pravdo, S. H., Serlemitsos, P. J., Swank, J. H., and Rothschild, R. H. 1978b, *Ap. J. (Letters)*, **226**, L65.
Mushotzky, R. F., Boldt, E. A., Holt, S. S., and Serlemitsos, P. J. 1979, *Ap. J. (Letters)*, **232**, L17.
Mushotzky, R. F., Marshall, F. E., Boldt, E. A., Holt, S. S., and Serlemitsos, P. J. 1980, *Ap. J.*, **235**, 377.
Mushotzky, R. F., Serlemitsos, P. J., Becker, R. H., Boldt, E. A., and Holt, S. S. 1978*a*, *Ap. J.*, **220**, 790.
Neugebauer, G., Oke, J. B., Becklin, E. E., and Mathews, K. 1979, *Ap. J.*, **230**, 79.
O'Dell, S. L., Puschell, J. J., Stein, W. A., Owen, F., Porcas, R. W., Mufson, S., Moffett, T. J., and Ulrich, M. H. 1978, *Ap. J.*, **224**, 22.
Osmer, P. S. 1978, *Ap. J. (Letters)*, **226**, L79.
Primini, F. A., *et al.* 1979, *Nature*, **278**, 234.
Readhead, A. C. S., Cohen, M. H., Pearson, T. J., and Wilkinson, P. N. 1978, *Nature*, **276**, 768.
Readhead, A. C. S., Pearson, T. J., Cohen, M. H., Ewing, M. S., and Moffet, A. T. 1979, *Ap. J.*, **231**, 299.
Redman, R. O. 1978, preprint.
Rees, M. J. 1978, *M.N.R.A.S.*, **184**, 61.
Ricketts, M. J., Cooke, B. A., and Pounds, K. A. 1976, *Nature*, **259**, 546.
Riegler, G. R., Agrawal, P. C., and Mushotzky, R. F. 1979, *Ap. J. (Letters)*, **233**, L47.
Rieke, G. H., and Weekes, T. C. 1969, *Ap. J.*, **155**, 429.
Rudnick, L., Owen, F. N., Jones, T. W., Puschell, J. J., and Stein, W. A. 1978, *Ap. J. (Letters)*, **225**, L5.
Scheuer, P. A. G., and Readhead, A. C. S. 1979, *Nature*, **277**, 182.
Schmidt, M. 1966, *Ap. J.*, **146**, 7.
Schreier, E. J., Feigelson, E., Delvaille, J., Giacconi, R., Grindlay, J., and Schwartz, D. A. 1979*a*, *Ap. J. (Letters)*, **234**, L39.
Schreier, E., Feigelson, E., Fabricant, D., and Gorenstein, P. 1979*b*, *Bull. AAS*, **11**, 791.
Schwartz, D. A., Bradt, H. V., Doxsey, R. E., Griffiths, R. E., Gursky, H., Johnston, M. D., and Schwarz, J. 1978, *Ap. J. (Letters)*, **224**, L103.
Schwartz, D. A., Doxsey, R. E., Griffiths, R. E., Johnson, M. D., and Schwarz, J. 1979, *Ap. J. (Letters)*, **229**, L53.
Schwartz, D., and Gursky, H. 1974, in *X-Ray Astronomy*, ed. R. Giacconi and H. Gursky (Dordrecht: Reidel), p. 359.
Setti, G. 1978, in *Pittsburgh Conference on BL Lac Objects*, ed. A. M. Wolfe (Pittsburgh: University of Pittsburgh), p. 385.
Setti, G., and Woltjer, L. 1979, *Astr. Ap.*, **76**, L1.
Sramek, R. A., and Weedman, D. W. 1978, *Ap. J.*, **221**, 468.
Swanenburg, B. N., *et al.* 1978, *Nature*, **275**, 298.
Tananbaum, H., *et al.* 1979, *Ap. J. (Letters)*, **234**, L9.
Turland, B. D. 1975, *M.N.R.A.S.*, **170**, 281.
Ulrich, M. H., Kinman, T. D., Lynds, C. R., Rieke, G. H., and Ekers, R. D. 1975, *Ap. J.*, **198**, 261.
Weedman, D. W. 1976, *Ap. J.*, **208**, 30.
———. 1977, *Ann. Rev. Astr. Ap.*, **15**, 69.
Worrall, D. M., Mushotzky, R. F., Boldt, E. A., Holt, S. S., and Serlemitsos, P. J. 1979, *Ap. J.*, **232**, 683.

ARIEH KÖNIGL: Theoretical Astrophysics, 130–33, California Institute of Technology, Pasadena, CA 91125